TAO, Vol.3, No.3, 277-292, September 1992

The Variability of Hydrographic Fields at Kuroshio's Turning on Northeast of Taiwan

JIAN-HWA HU[1] and JIA-LEH CHANG[2]

(Received: February 20, 1992; Revised: July 10, 1992)

ABSTRACT

The empirical orthogonal functions analysis is applied to the time series of monthly hydrographic sections across Kuroshio near northeast of Taiwan. The EOF's of the first three modes account for 50-70% of the total variabilities. Physical processes revealed are cycles of the seasonal thermocline and halocline due to solar heating and shift of Kuroshio axis, the baroclinicity due to change of Kuroshio geostrophic velocity, the frontogenesis between East China Sea water and Pacific Ocean water due to orthogonal components of monsoon, and the upwelling induced by current geostrophy instead of the continental slope effect.

1. INTRODUCTION

Initiated by the North Equatorial Current (NEC), Kuroshio carries warm and saline water flowing towards the north. After passing Bashi Channel, it basically moves along the east coast of Taiwan where the continental shelf is narrow and the slope is steep. Hu (1991) in a study of TOGA mixed-layer drifters hypothesized that the northeast monsoon since October is the major mechanism to significantly disturb/slow the surface Kuroshio system and cause the well-known bifurcation in winter over the Channel (Nitani, 1972). The same wind system was also assumed to render Kuroshio the narrowest and possibly the strongest in a year during February and March. Drifter trajectories (Figure 1) also illustrate the variation of surface flows in different seasons at northeast of Taiwan where Kuroshio turns to skirt along the isobath of 200m continental break (Figure 2). A model to study the flow pattern over this region was reported by Chao (1991).

A main interest in this area is to understand the complex of the confluence and exchange of Kuroshio water, East China Sea (ECS) water and Taiwan Strait water. For instance, a local cold water mass was frequently observed (Fan 1980; Chern *et al.*, 1990), while its forcing has not been convincingly clarified. Among some points of view, the bottom topography is generally believed to be important (e.g., Wong *et al.*, 1991). To approach this uncertainty, an intensive oceanographic survey was thus conducted under the Kuroshio Edge Exchange

[1] Department of Oceanography, National Taiwan Ocean University, Keelung, Taiwan, R.O.C.

[2] Hydrology and Marine Division, Central Weather Bureau, Taipei, Taiwan, R.O.C.

Processes (KEEP) project. This paper is to study the spatial and temporal variabilities of the hydrographic fields by analyzing their principal components.

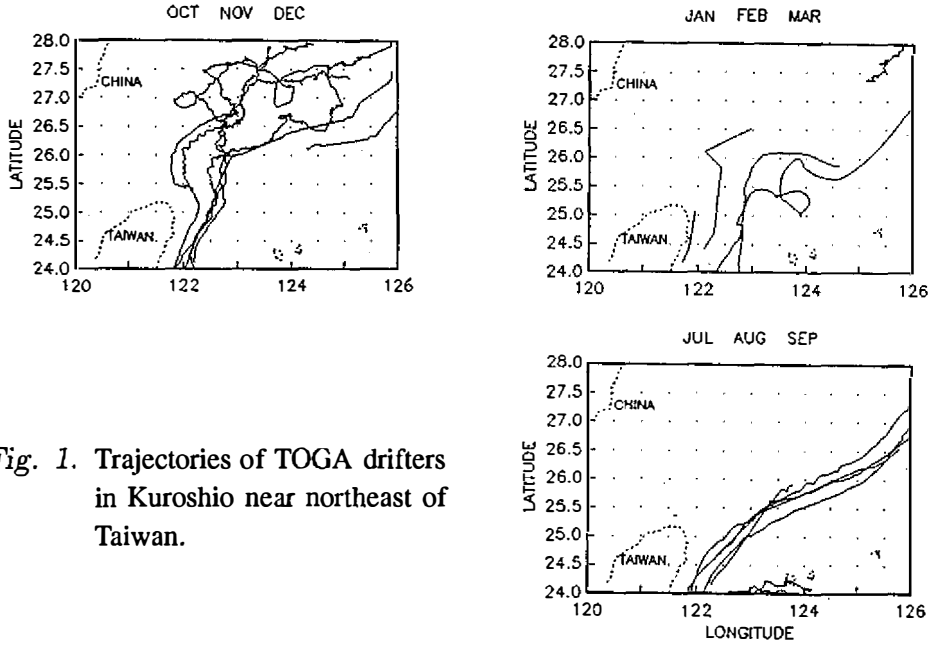

Fig. 1. Trajectories of TOGA drifters in Kuroshio near northeast of Taiwan.

2. KEEP HYDROGRAPHIC EXPERIMENTS

A monthly survey along a track which surrounds the cold dome region at the northeast of Taiwan was designed for the KEEP Project (ref. KEEP NEWSLETTER, Vol. 3). This track has two major transects, A and B, both across Kuroshio (Figure 2). Along the track a total of 21 stations were pre-set for routine observations, in which measurements of CTD rosette provided the fundamental data base of the hydrography. The distance between two stations is about 14 miles, excluding the two supplementary stations (A5b and B4b) near the continental shelf break at a water depth of about 200m. Station B0 is not on either transects and therefore its data are not included in this study. Station A9 is so chosen since the extension of transect A at position 24°30′N, 122°50′E will be in the territorial waters of the Japanese Yonaguni Island.

This report basically employs the time series data on the two KEEP P-Box CTD transects conducted by R/V Ocean Researcher I of the Republic of China. Prior to the first KEEP P-Box survey in August of 1990, two more CTD measurements along the same track were made by the author in June and July with R/V Hifu of Institute of Fishery Department, R.O.C.. The monthly KEEP P-Box survey ended in July of 1992. However, there was no observation in February due to ship's annual maintenance. Both of the two transects of the last July cruise and transect A of December cruise could not be surveyed due to weather constraints. The total numbers of months with available CTD data thus become 12 for transect B and 11 for A. Details of P-Box surveys are listed in Table 1. The CTD data were compared with Autosal readings, showing an accuracy agreeing with the reported value of SeaBird CTD model SBE-9.

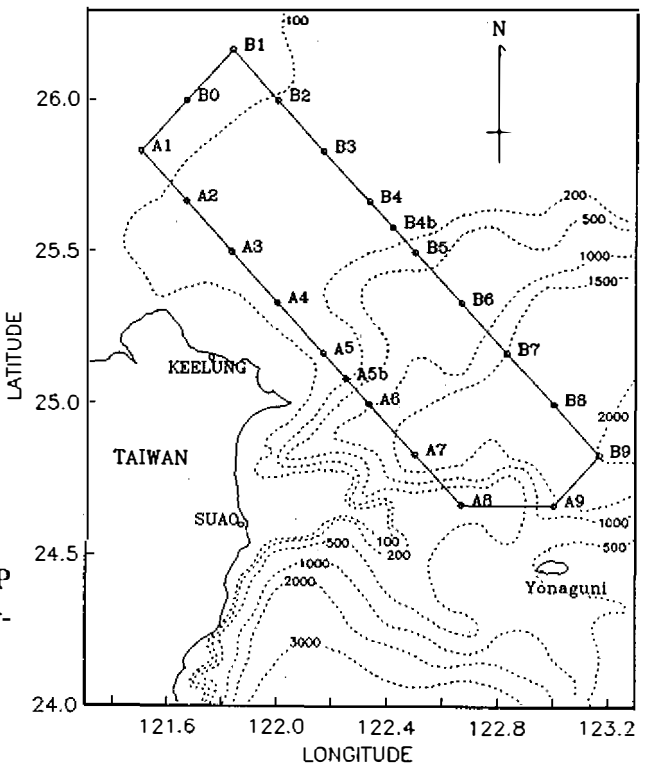

Fig. 2. Bottom topography of KEEP region and KEEP P-Box survey transects.

Table 1. KEEP P-Box hydrographic surveys in 1990-1991

P-Box cruise	date	R/V	Remarks
Jun. 1-5,	1990	Hifu	No A5b and B4b
Jul. 2-6,	1990	Hifu	No A5b and B4b
Aug. 1-6,	1990	OR 1	
Sep. 18-23,	1990	OR 1	
Oct. 10-25,	1990	OR 1	
Nov. 3-7,	1990	OR 1	
Dec. 3-7,	1990	OR 1	No transect A
Jan. 11-15,	1991	OR 1	No A1,A5b,A6.
Mar. 4-9,	1991	OR 1	
Apr. 1-6,	1991	OR 1	
May 2-7,	1991	OR 1	
Jun. 7-12,	1991	OR 1	

OR : Ocean Researcher

3. THE HYDROGRAPHIC FIELDS AND THEIR VARIATIONS

The time series of temperature and salinity sections at both transects A and B are prepared from averaged data of every 10m in Figures 3 and 4. Data below 600m depth are excluded because of less importance in their small variation. The cross marks in the figures represent where there was no data and interpolation is applied for contouring.

From these figures, many phenomena are observed. First of all, the seasonal thermocline is shaped by currents, including the consistent northward Kuroshio in deep water region and the occasional reversed flow in the continental shelf region or near the slope, to form a cold dome. This statement implies that the dome could be geostrophically determined; it is also thought to be the result of an upwelling when deep water is forced up by the continental shelf due to current impact (Wong *et al.*, 1991). They might not be the same mechanism. The former deals with current speed, while the latter relates to current direction.

Nevertheless, seasonal variation of the thermocline is obvious. The thermocline was rigid and covered the region from shelf to deep water in warm seasons; while for cold seasons it was weak, even disappearing in the shelf region in March. However, to conclude how the associated cold dome varied from time to time is not attainable, although some well-depicted domes can be identified from November to January. We compared the cold core shown in SST images (provided by Hsu *et al.*, 1991) to the subsurface temperature field. No general relation was found either, indicating the difficulty of cold dome study.

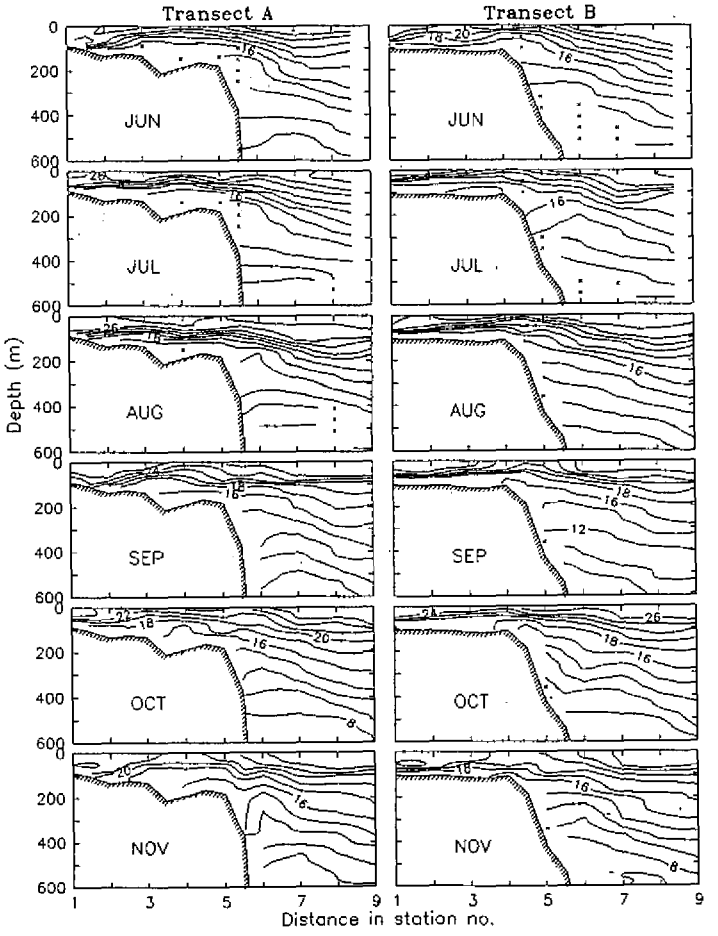

Fig. 3. Time series of temperature sections at transects A and B.

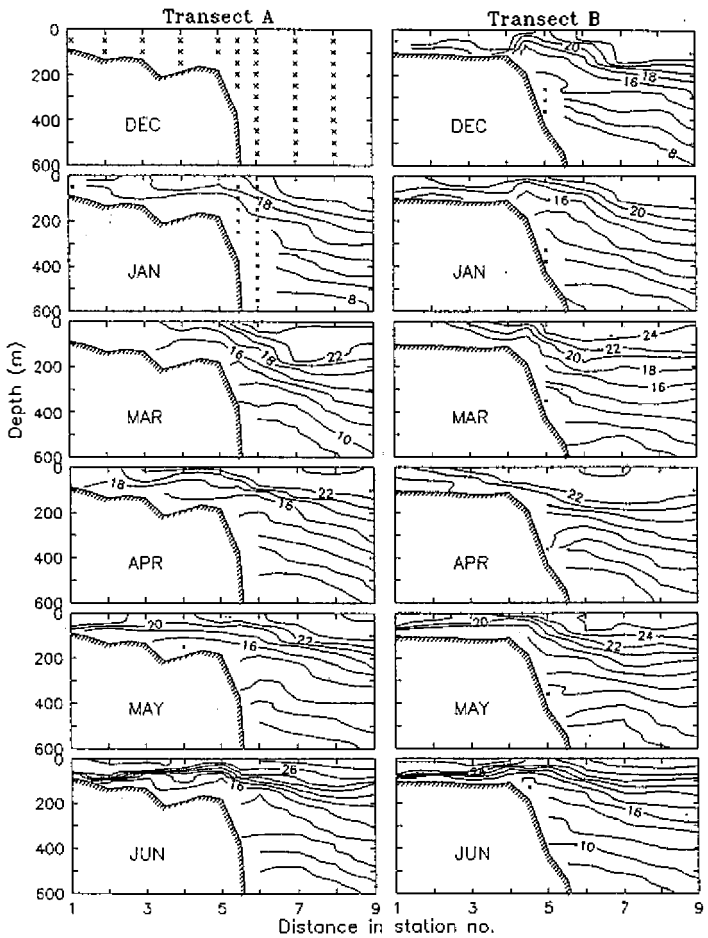

Fig. 3. (Continued)

On the other hand, seasonal halocline is also observed but with its variation from one month to another not as smooth as for thermocline. For instance, the summer halocline disappeared in October, but returned in November when the low salinity ECS (East China Sea) water intruded from north (water between Stations 1-3) and spread over the top layer of the region. The same ECS water appeared again in March to form a strong halofront but with small ranged temperature in the whole water column over the shelf (Figure 3), meaning that the water was actually not well mixed.

The appearance of ECS water thus throws some light on how the summer halocline was formed. Namely, the surface less saline water from July to September originated from the ECS as well. Drifter trajectories in these months (Figure 1 bottom panel) depict a rather non-diverged surface flow pattern. This pattern suggests that Kuroshio main stream was passing through Stations 7-9, leaving the west of the stream characterized by ECS water. During other months (drifter data for April to June are not available yet), Kuroshio intruded the shelf region and diverged before it turned into a northeast flow. This motion would bring in water of higher salinity from open ocean to the shelf region. This phenomenon is also

indicated by the lateral movement of the subsurface high salinity core (above 300m between Stations 6-9) across the shelf break as Figure 4 shows.

These are mechanisms or effects obviously contributing to the perturbation of the hydrographic fields. There could be some more that we are not able to identify easily. To more quantitatively identify each individual process, a further study is required. We thus apply the following method.

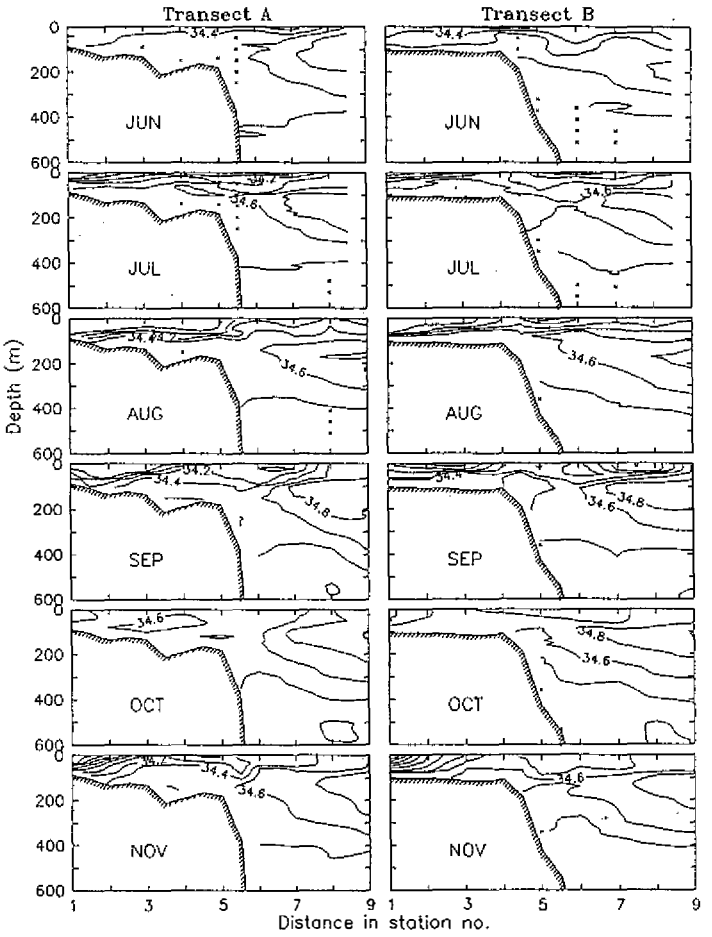

Fig. 4. Time series of salinity sections at transects A and B.

4. PRINCIPLE OF EMPIRICAL ORTHOGONAL FUNCTIONS ANALYSIS

A convenient and effective tool for summarizing the spatial and temporal variabilities of the hydrographic data set is to display the empirical orthogonal functions (EOF's) of the temporally averaged spatial correlation matrix. The EOF's theory and technique are well documented and widely discussed (e.g., Lorenz, 1956; Weare, 1977; Preisendorfer, 1988). Here we will make our effort mainly to present and discuss the results in terms of physical processes which might lead to their variability.

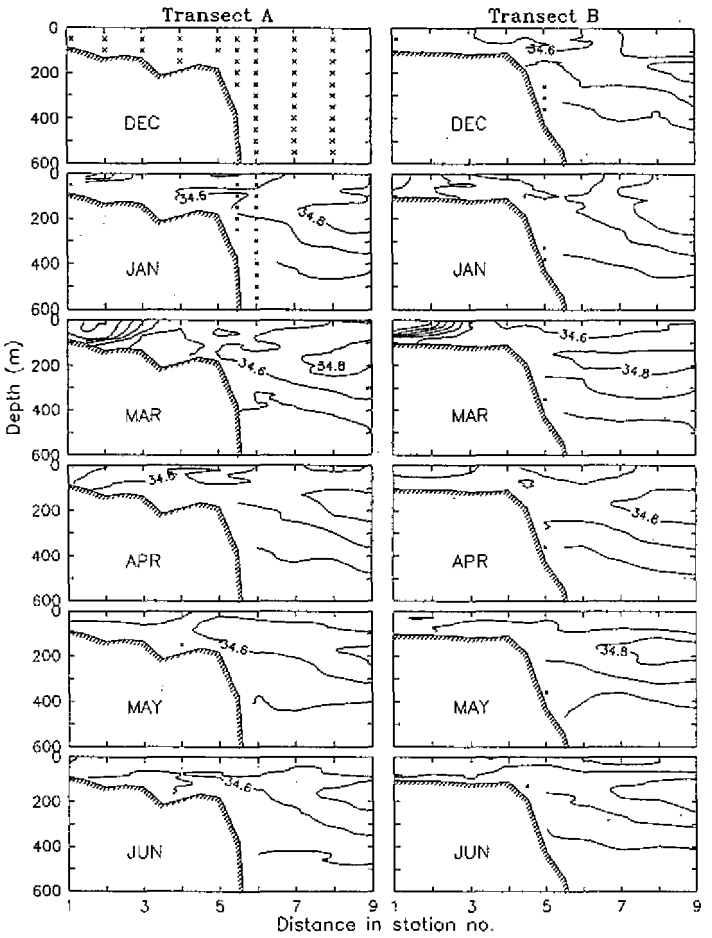

Fig. 4. (Continued)

In our presentation, the EOF's are ranked by the amount of variance each accounts for over the entire domain. Alternate rankings can be sought, for example, to display the ranked order which accounts for the variance of a particular feature or variance at a particular location. In our analysis an EOF is a spatial distribution function, scaled to unit variance over the spatial domain. To obtain its contribution to the variance at any particular time, we multiply it by the dimensional amplitude modulation in time — the eigencoefficient. Namely, in brief, for a time series of a field F(τ), τ=1$\rightarrow$n, n is a finite number,

$$F(\tau) = \bar{F} + \sum_{M}^{\infty} p_M(\tau) f_M(\tau) F_M \tag{1}$$

where $\bar{F}$ is the mean field, p_M is the proportion of contribution the eigenfunctions account for at certain τ to the total variability for the M mode, $f_M(\tau)$ is the time series of eigencoefficients for each M mode, and F_M is the eigenvector for the M mode. The total variance percentage accounted for by each mode is

$$P_M = \sum_{\tau=1}^{n} p_M(\tau) \tag{2}$$

Since the EOF's of higher modes account for less percentage of total variance and are therefore of less significance, only the first three modes will be discussed. We denote the EOF's in space domain, i.e. the eigenvectors of the first three modes as T1, T2, T3, S1, S2, and S3, for temperature and salinity fields respectively. The corresponding time series of eigencoefficients are denoted in lower case letters as t1, t2, t3, s1, s2, and s3.

5. PRINCIPAL COMPONENTS OF THE VARIABILITIES

In the EOF's analysis, the mean field and its total variance (or standard deviation) are derived first. The standard deviation of a field is denoted by a tilde in this paper, i.e., $\tilde{T}$ and $\tilde{S}$. Figure 5 illustrates the results.

The similarity between the mean fields at two transects is much higher than that between individual monthly observations (Figures 3 and 4). In Figure 5 both main thermocline and halocline are delineated. The contrast of the subsurface high salinity core in deep water region to the surface low salinity ECS water in continental shelf region makes up the main feature of the mean salinity field. These two waters are separated by mean Kuroshio and the cold dome suggested by the $\bar{T}$ sections. Notice that the isotherms in the high salinity core are rather flat, implying a relatively weak flow at there.

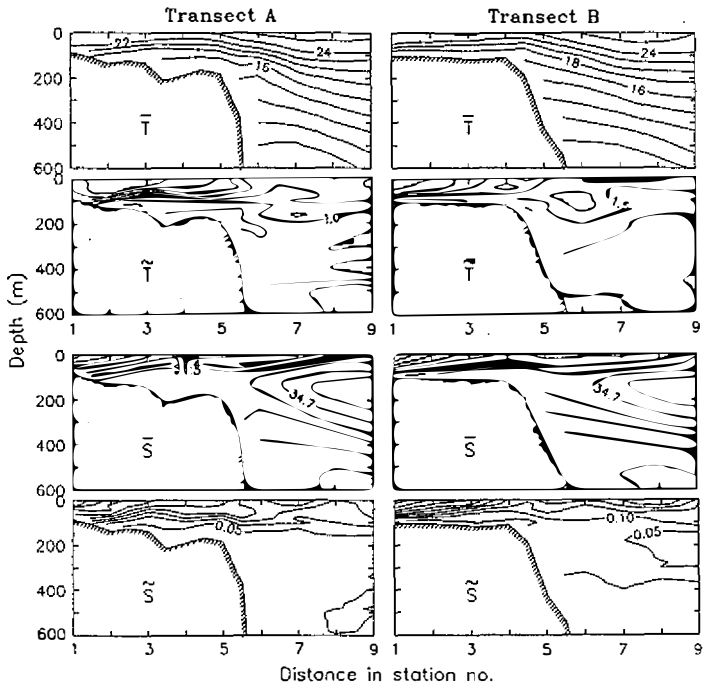

Fig. 5. Means and total variances of temperature and salinity fields.

The $\tilde{T}$ and $\tilde{S}$ sections display a general pattern of variance decreasing from surface to bottom with maxima occurring at ECS water front. Local high of $\tilde{T}$ can be found at a depth of 100-200m around Stations 5-7, where is located the thermocline of the greatest lateral slope, a strong or main flow implied. The second halocline beneath the saline core is relatively stable, indicated by the low $\tilde{S}$.

By decomposing the total variance into principal components, the EOF's of the first three modes are illustrated in Figure 6 (for T field) and Figure 7 (for S field). These figures are arranged such that each eigenvector is associated with its eigencoefficient series. The coefficients of December at transect B are duplicated in the plots of time series at A to avoid too much bias if a linear interpolation is applied. Dotted segments in the t and s series around December at transect A represent the suggestion from data at transect B. The percentage of total variance accounted for by each mode is printed in the eigenvector panel for reference.

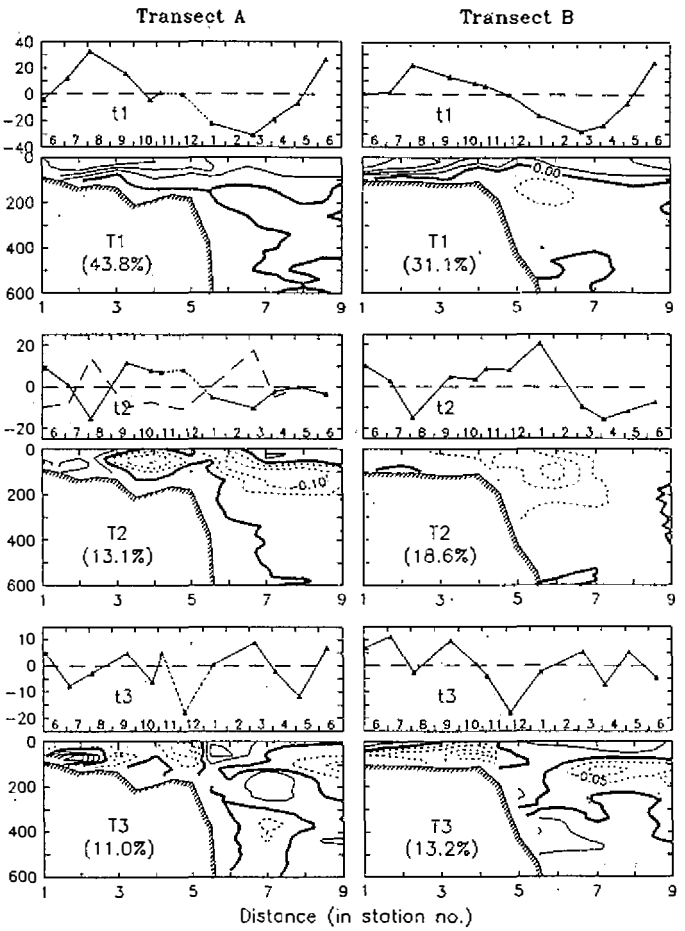

Fig. 6. EOF's of temperature field for the first 3 modes. See text for the dashed curve in t2(A) panel.

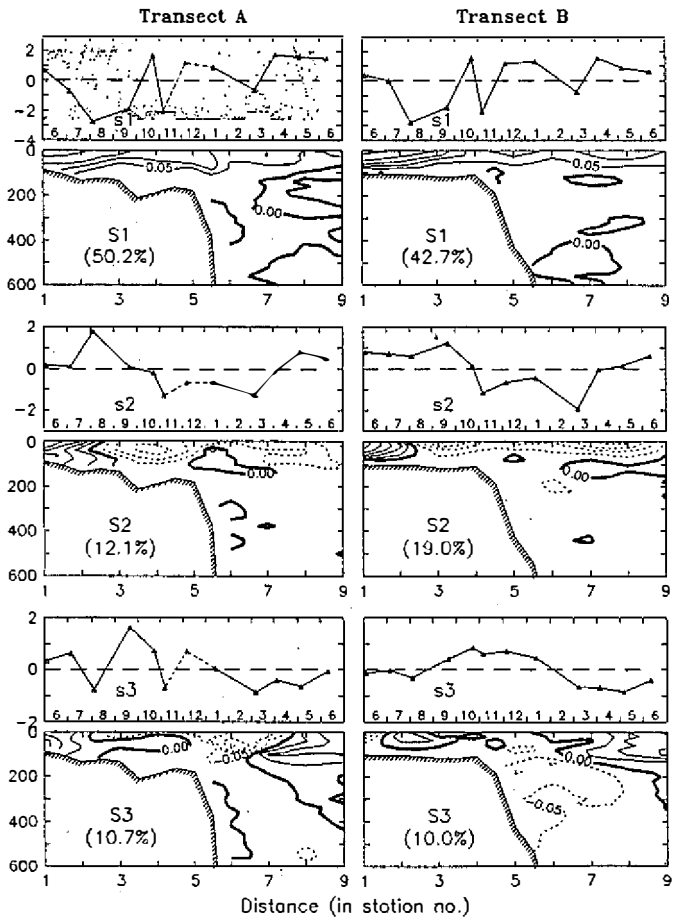

Fig. 7. EOF's of salinity field for the first 3 modes. See text for the dots in s1(A) panel.

5.1 Temperature Field

T1 patterns basically resemble those of $\tilde{T}$ above 100m, although they account for about only 31-44% of the latter. The generally horizontal distribution of the in-phase (all positive) isopleths with values decreasing downward suggests an approximately equal weight of an influence from the surface into the water over the whole region. The annual cycle in t1 series with high in summer (Eq.1 thus means an increase of temperature to the mean field) and low in winter provides the answer that the forcing must be the solar heating. The small positive/negative values of T1 below 100m simply represent the insignificance of the forcing down there.

Nevertheless, there is a slightly significant negative T1 with a contour of -0.05 at a depth about 100m at transect B and also the upward convexity of contour lines (meaning a low) at about 100m of Stations 6-7 at transect A, just corresponding to the local high in $\tilde{T}$ where the main stream of Kuroshio perhaps passed through. We tentatively interpret it as meaning that solar heating can be affected by mixing of a strong current.

T2 patterns between transect A and B do not resemble each other as much as for T1. T2(A) has two extremes, while T2(B) has one. The amount of variance this mode accounts for at B (19%) becomes greater than at A (13%). However, the general trends of t2 at both transects are about the same, i.e., low in August and cool months. To postulate a related physical process needs to invoke the computation of Eq.1. The result can be conceptually explained as the following.

Let's arbitrarily consider the case of negative t2 in August. For the portion with negative T2, the temperature of the mean field (Figure 5) will be increased by an amount depending upon p2 of August and the contour of T2. Thereby, for a certain value of p2, the isotherm of a particular temperature would descend more where the temperature increases more. The T2 contour thus causes the inclination of the isotherm near the main flow steeper than at previous time for both transects; for transect A, a similar result also happens on the shelf side of the cold dome. Such a process should intensify or weaken (for +t2) the baroclinic condition of the flow, implying a change of current geostrophic velocity.

Station pairs of 6-7 and 7-8 at transect A were chosen to derive the geostrophic profiles with respect to 1000m. The time series of the averaged velocites in upper 300m is also plotted in t2(A) panel as the dashed curve, in which zero t2 represents 70 cm/sec and 1 unit of t2 equals 2cm/sec. The correspondence of negative t2 to high geostrophic flow is evidenced. We thus conclude that Kuroshio geostrophic velocity was the second factor to determine the temperature variability of the field.

T3 contributes slightly less amount of variance to the total as does T2. The P_M in Eq.2 for $M > 3$ drops drastically down to 5% or less with complicated eigenvectors. They are hence thought to be noises. Both T3 patterns are getting complicated to understand, even a computation of Eq.1 for this particular mode cannot provide a clue. In addition, the dissimilarity between t3(A) and t3(B) and their irregularity also leads to the same idea of little significance as for higher modes. We thus leave the diagrams for comparison when the third mode of salinity field is discussed below.

5.2 Salinity field

S1 accounts for about 43-50%, near one half of $\tilde{S}$, higher than T1 does. The resemblance between S1 and $\tilde{S}$ is thus not a surprise; while the striking feature becomes the resemblance between S1 and T1 in upper layer to a high extent, mystifying if they are under the same physical process. The signal from s1 series is by no means related to t1. Such a significant variation of salinity during a year is also hardly a result of direct solar heating. Comparing the sequence of diagrams in Figure 4, it becomes clear how and what s1 series accounts for. That is as introduced in Section 3, the variation of main halocline due to presence of ECS fresher water together with the lateral back-and-forth motion of the subsurface saline core. The question remained is as to why s1 varied so.

In the s1(A) panel, daily averaged wind direction data are also shown as dots. For this, the vertical axis of the panel is scaled equivalent to -50° to 300°; i.e., each tick mark represents a 50° increment. It is seen that the peak of s1 in October is likely to be a quick response of Kuroshio in upper layer to the onset of northeast monsoon; namely, the westward forcing shifted the current to the continental shelf as Figure 1 (top panel) shows. And then, as recently suggested by Y. Hsueh (1992, personal communication), a high pressure might occur immediately on the shelf of ECS. The ECS water thus returned to the shelf transiently in November (after about 10 days, see Table 1) before a new equilibrium state was reached.

As to the returning of ECS water in March, a different mechanism was functioning. First indication is in Figure 3(b) (March panel), the ECS water had a small temperature range

between 16°-18°C unlike the stratification near bottom in November case. The second is in Figure 1 (middle panel), the southwest shift of drifter trajectories in this area during the season. And the third is in Figure 6 (dashed curve in t2(A) panel), the current persistently intensified since January and reached its zenith to gain a speed of over 100cm/sec in March. This process hence may simply mean that a current of high momentum may straighten its curved flow in low speed, and therefore bring the water volume away from the site of curved motion. In other words, the ECS water was pulled back by Kuroshio intensification since January until the extreme in March. The sharp surface halofront near Station 3 kept the fresher water away from the top layer of Kuroshio, explaining (1) the westward forcing of northeast winds superimposed against the eastward pulling to build up the sharp front and (2) the absence of ECS water in Kuroshio made s1 of March much smaller than of November in magnitude.

According to drifter study, an explanation of Kuroshio's intensification from January to March was suggested by Hu (1991). In brief, the momentum of Kuroshio is gradually enhanced by the intensified North Equatorial Current under northeast monsoon. After March, wind system altered to be generally southeast while the jet of Kuroshio exhausted its excess momentum. The ECS water was thus removed again by northward forcing of winds together with the possible diverged Kuroshio as indicated in Figure 4. The equilibrium state stayed for a few months until the summer jet was formed to bring ECS water back. However, on the contrary, the eastward forcing of the winds distributed the ECS water over the top of Kuroshio.

S2 accounts for 12-19% of $\tilde{S}$, mainly characterizing the variability of upper layer as T2. The major feature of the out-of-phase S2 pattern is the contrast of waters in ECS domain and rest of the region (we thus name it the Kuroshio domain). Namely, this mode distinguishes the reversed response of water salinity in two domains from the overall spreading or retreating of ECS water accounted for by S1 mode. The mechanism is very possibly the forcing by north-south components of winds hinted by t2 series which fairly well show the monsoon annual cycle altering in October and April. In detail, when northeast monsoon prevailed (negative s2), the Kuroshio domain was getting saltier as discussed already; while by some chance the ECS fresher water would be forced southward into the ECS domain of the region. Southwest monsoon is also successfully applied for reversed response. As to whether that p2(B)>p2(A) while p1(B)<p1(A) for both T and S fields is merely a coincidence or the fundamental difference between the two transects is uncertain at present.

S3 accounts for even less amount of $\tilde{S}$, but somewhat resemble between its two patterns at transects A and B. Furthermore, the annual cycle of s3 at transect B is hardly a phenomenon of noise, even though s3(A) shows differently. However, the cycle implys a freshening of Kuroshio main flow occurred from surface to great depth in fall and winter (at transect B only), while portions of some shelf water and the saline core were getting saltier. A possible process that can be thought of is the upwelling of deep, less saline water in the current, which also lifted the saline core and water on shelf up or away to increase the salinity around there. This upwelling could be due to the variation of geostrophic condition because a rough similarity between s3 and t2 is found if the sign is not considered seriously; i.e., the tendency of curves to go up or down is considered when the agreement of sign is not valid. The domination of S3(A) in the upper layer together with the mild out-of-phase response along the continental slope could be also due to bottom topography. As shown in Figure 2, transect A is closer to the shallow (<200m) Suao Ridge and the north coast of Taiwan than transect B. The water in the shadowed deep basin right behind the Ridge might not be removed or filled in as freely as where transect B is located.

6. SUMMARY AND CONCLUSION

The one year monthly CTD surveys along two transects across Kuroshio near northeast of Taiwan provide an opportunity to understand better how various physical processes interactively govern the current. The method applied is to decompose the hydrographic variability into principal components. In the temperature field, the major process must be the variation of seasonal thermocline which accounts for the total variance for more than double of the next processes. The second process is very likely to be the geostrophic response when Kuroshio varies its speed. We did expect to see a process of upwelling due to the effect of continental slope when Kuroshio shifts towards the shelf. However, in the temperatue field, we are not able to resolve it. 50% of total temperature variance are accounted for by the above processes.

On the other hand, the major process in the salinity field is the variation of main halocline due to the lateral shift of Kuroshio axis under the east-west forcing of monsoon. It induces the back-and-forth motion, thus the exchange, of the ECS fresher water and the open Pacific high salinity water in upper layer. The evidence of Kuroshio shift from drifter tracks and the hydrographic fields quite agree with each other. However, the two waters may not always completely dominate the top layer by terms because the north-south components of monsoon would also force the ECS water against the lateral shift of Kuroshio, creating a halofront on the shelf. This is the second process to vary the field in an out-of-phase manner. While the third mode of salinity field surprisingly implies the process of upwelling in Kuroshio, but mainly due to the geostrophic reason as for second mode of temperature field. The amount of total salinity variance accounted by the processes discussed here is more than 70%.

Acknowledgements This study was supported by National Science Council of R.O.C. with project number NSC81-0209M019-06. CTD data were collected by scientists who participated in the KEEP project. Without their collaboration, this study could not be done. We are also thankful to all cruise personnel for their regular monthly services. The first draft of this paper was written during the one-month cruise of R/V Polar Duke for RACER Program in Antarctica, a silent and chilly place but abundant in imagination for writing.

REFERENCES

Chao, S.-Y., 1991: Circulation of the East China Sea, A numerical model, *J. Oceanogr. Soc. Jpn.*, **46**, 273-295, 1990.

Chern, C.-S., J. Wang and D.-P. Wang, 1990: The Exchange of Kuroshio and East China Sea Shelf Water, *J. Geophys. Res.*, **95**, 16017-16023.

Fan, K.-L., 1980: On Upwelling off Northeastern Shore of Taiwan, *Acta Oceanogr. Taiwan*, **11**, 105-117.

Hsu, T.-J., C.-Y. Lin and W.-H. Shih, 1991: Study on Satellite SST Images during the KEEP Hydrography Survey Periods in 1991-1992. KEEP Newsletter, Vol. 8.

Hu, J.-H., 1991: The Past, Present and Future of Kuroshio's Drifter Observations, Workshop on Physical and Chemical Oceanographies in Ocean and Seas Near China, Hongzhou, China, 25-29 June 1991.

——— 1991: WOCE/TOGA Surface Velocity Programme, Planning Committee, Report of the 3rd Meeting with focus on the Pacific Sector. WOCE Report No. 65/91.

Lorenz, E.N., 1956: Empirical Orthogonal Functions and Statistical Weather Prediction, Scientific Report No.1 of Dept. of Meteorology of M.I.T., 49pp.

Nitani, H., 1972: Beginning of the Kuroshio, Univ. of Washington Press, Seattle and London.

Preisendorfer, R.W., 1988: Principal Component Analysis in Meteorology and Oceanography, Elsevier, Amsterdam, 425pp.

Weare, B.C., 1977: Empirical orthogonal analysis of Atlantic Ocean surface temperature. *Q. J. R. Meteorol. Soc.*, **103**, 467-478.

Wong, G., S.-C. Pai, K.-K. Liu, C.-T. Liu and C.-T. Chen, 1991: Variability of the Chemical Hydrography at the Frontal Region between the East China Sea and the Kuroshio Northeast of Taiwan, Estuarine, *Coastal and Shelf Science*, **33**, 105-120.

臺灣東北角黑潮轉向處之水文場變化性

胡健驊
國立海洋大學海洋科學系

張迦勒
中央氣象局水文海洋氣象科

摘要

橫截臺灣東北角海域黑潮每月所量測的水文時間序列資料以經驗正交函數(EOF)方法分析，前三階即闡述了總變化量的50-70%，所揭示的物理過程有因太陽入射能量及黑潮主軸變動所引發的斜溫層及斜鹽層之季節性週期，有因黑潮地轉流的改變所影響的斜壓性，有因季風正交分量所帶動的中國東海水及太平洋海水間的成鋒過程，還有因洋流的地轉性而非一般所咸信的大陸坡效應所衍生的湧升現象。